## Technical University of Denmark

DTU

# Terahertz-induced Kerr effect in amorphous chalcogenide glasses

**Zalkovskij, Maksim; Strikwerda, Andrew; Iwaszczuk, Krzysztof; Popescu, A.; Savastru, A.; Malureanu, Radu; Lavrinenko, Andrei; Jepsen, Peter Uhd**

## DTU Library
Technical Information Center of Denmark

# Terahertz-induced Kerr effect in amorphous chalcogenide glasses

M. Zalkovskij, A. C. Strikwerda, K. Iwaszczuk, A. Popescu, D. Savastru, R. Malureanu, A. V. Lavrinenko, and P. U. Jepsen
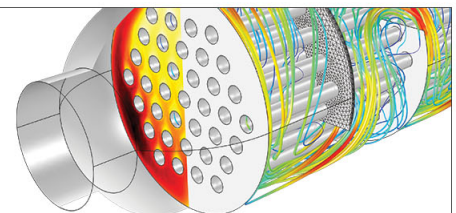
# Terahertz-induced Kerr effect in amorphous chalcogenide glasses

M. Zalkovskij,[1,a)] A. C. Strikwerda,[1] K. Iwaszczuk,[1] A. Popescu,[2] D. Savastru,[2]
R. Malureanu,[1] A. V. Lavrinenko,[1] and P. U. Jepsen[1]

[1]*Department of Photonics Engineering, Technical University of Denmark, Kgs. Lyngby, DK-2800, Denmark*
[2]*National Institute of R&D for Optoelectronics INOE 2000, Bucharest, Romania*

We have investigated the terahertz-induced third-order (Kerr) nonlinear optical properties of the amorphous chalcogenide glasses $As_2S_3$ and $As_2Se_3$. Chalcogenide glasses are known for their high optical Kerr nonlinearities which can be several hundred times greater than those of fused silica. We use high-intensity, single-cycle terahertz pulses with a maximum electrical field strength exceeding 400 kV/cm and frequency content from 0.2 to 3.0 THz. By optical Kerr-gate sampling, we measured the terahertz-induced nonlinear refractive indices at 800 nm to be $n_2 = 1.746 \times 10^{-14}$ $cm^2/W$ for $As_2S_3$ and $n_2 = 3.440 \times 10^{-14}$ $cm^2/W$ for $As_2Se_3$. © 2013 AIP Publishing LLC.
[http://dx.doi.org/10.1063/1.4832825]

Terahertz (THz) technology has the potential for application in a broad range of fields, e.g., biology, medicine,[1] communication, and in the space-, defense-, and semiconductor-industry.[2,3] While there has been tremendous progress in the development of THz sources, detectors, and passive linear components, many applications, such as ultrafast all-optical signal processing, require more versatile, nonlinear components. To construct these nonlinear components, materials with nonlinear interactions between the THz electric field and matter must be identified, developed, and quantified.

Chalcogenide glasses, first reported six decades ago,[4] have attracted significant attention in recent years due to their unique properties such as high refractive index, mid-infrared transparency, and very large third-order (Kerr) non-linearity.[5] Their large nonlinearities in the optical, near-, and mid-infrared regions have made them promising candidates for fast nonlinear optical devices.[6]

The measurement of the THz-induced optical Kerr effect in solid-state materials has traditionally been hampered by a lack of high intensity THz sources. However, the recent introduction of tilted pulse front THz generation in lithium niobate ($LiNbO_3$)[7] now makes THz field strengths of the order of 1 MV/cm available.[8,9] Such pulses were recently applied for the investigation of the THz-induced optical Kerr effect in liquids[10] and in relaxor ferroelectrics.[11]

In this paper, we report the observation of the THz-induced optical Kerr effect in two bulk, amorphous chalcogenide glasses, $As_2S_3$ and $As_2Se_3$, and determine their third-order nonlinear coefficients. Both glasses have become very popular in optics due to their high nonlinear coefficients[12–15] and flexibility towards micro- and nano-fabrication.[16–18]

Our experimental setup is shown schematically in Fig. 1(a). Briefly, an amplified femtosecond laser system (pulse energy 3.5 mJ, duration 100 fs, center wavelength 800 nm) drives a standard tilted pulse front scheme for generation of intense THz pulses in $LiNbO_3$.[8] The generated THz beam is tightly focused onto the sample by a combination of off-axis paraboloidal mirrors. A small portion of the 800 nm laser beam is picked off prior to the $LiNbO_3$ crystal and used to sample the THz-induced birefringence in the chalcogenide samples (0.716 mm thick $As_2S_3$ and 1.059 mm thick $As_2Se_3$) in a Kerr-gate sampling configuration. The temporal shape of the Kerr signal is recorded by gradually delaying the optical probe beam with respect to the THz beam while monitoring the THz-induced birefringence. In order to determine the absolute field strength of the THz pulses, the chalcogenide samples were replaced by an 300 μm thick electro-optic gallium phosphide (GaP) crystal so that the temporal profile of the THz pulses could be measured by electro-optic (EO) sampling.[19–21] The detected THz pulse is shown in Fig. 1(b) and has a peak electric field strength of 400 ± 10 kV/cm. This number is a minimum value, and is determined by EO sampling via the recorded phase retardation and its relation to the absolute electric field strength, $\Delta\phi = \omega L n_0^3 r_{41} E_{THz}/c$, where $r_{41}$ is the electro-optic coefficient, $n_0$ is the refractive index at the probe wavelength ($\lambda = 2\pi/\omega$), and $L$ is the length of GaP crystal.[22] During electro-optic sampling, the THz signal was attenuated by a number of high-resistivity silicon wafers in order to avoid over-rotation, and the attenuation from the wafers was subsequently accounted for in the field calibration. The frequency content spans the 0.05–3 THz region with 84% of the pulse energy concentrated within 0.2–1.0 THz. The alignment, and thus spatial overlap of generation and probe beam paths, was unchanged during both the Kerr characterization of the chalcogenide samples and the electro-optic sampling of the pulse shape.

In the Kerr-gate experiment, the probe beam is initially polarized at 45° with respect to the THz pulse polarization while in EO sampling experiments the probe beam is parallel with THz pulse polarization. The THz-induced phase difference, $\Delta\phi$, between the two polarization components parallel and perpendicular to the THz field polarization is detected as a differential voltage relative to the unperturbed signal on each photodiode. This signal, which is measured after propagation through a quarter-wave plate and polarizing beam splitter in a standard balanced scheme,[10] can be modeled as $\Delta V/V_0 = \sin(\Delta\phi) = \sin(\Delta n \omega L/c)$. Here, $\Delta n$ is the THz-induced modulation of the refractive index, $\omega$ is the angular
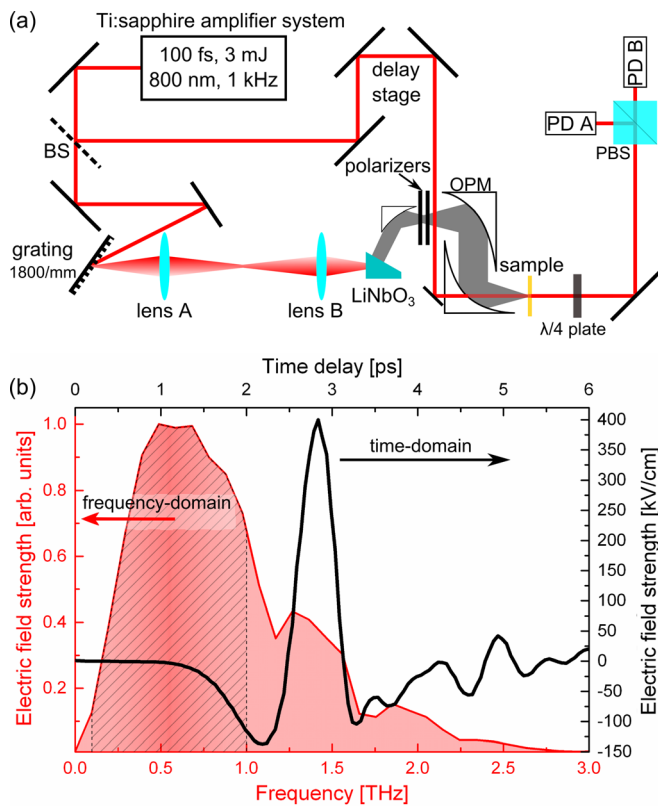
a)Electronic mail: mzal@fotonik.dtu.dk.

FIG. 1. (a) A schematic illustration of the $LiNbO_3$ THz-TDS system used for THz Kerr measurements. (b) THz pulse in time- (black curve) and frequency-domain (red curve). 84% of the pulse energy is concentrated between 0.2 and 1.0 THz, and is highlighted by dashed area. (BS) beam splitter, (OPM) optical parabolic mirror, (PD) photodiode, and (PBS) polarizing beam splitter.
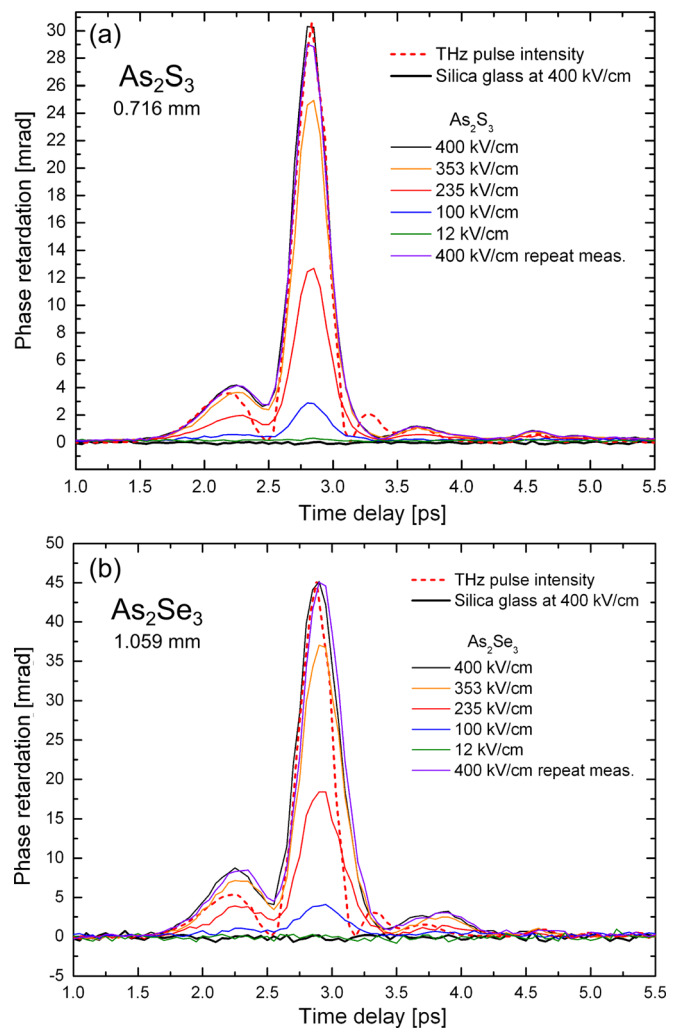


FIG. 2. The THz-induced birefringence in (a) $As_2S_3$ (0.716 mm) and (b) $As_2Se_3$ (1.059 mm) bulk samples as a function of the peak THz field strength. The intensity of the THz pulse normalized to the maximum recorded signal is indicated by the dashed, red curve. The black curve is for a 1 mm thick silica glass sample measured with 400 kV/cm field strength for comparison.

frequency of the probe beam, and $L$ is the effective propagation length in the crystal. The probe beam intensity was kept at a low level to avoid any photodamage to the samples.

The recorded Kerr probe signals in $As_2S_3$ and $As_2Se_3$ at varying THz field strengths are shown in Fig. 2. The field strength was attenuated by a pair of wire grid polarizers placed immediately after the first paraboloidal mirror. To verify that the samples were not damaged during the characterization, each sample was measured at the highest field strength both at the beginning and at the end of the measurement series. The results were then compared to confirm that the samples had not been damaged during the characterization. As expected, the recorded signal increases with the THz pulse strength. At a field strength of 47 kV/cm, the THz-induced signal is barely noticeable but it grows significantly at higher field strengths. We used a 1 mm thick bulk silica glass sample as a reference. Even with the full field strength (400 kV/cm), no THz-induced birefringence was observed due to the very small third-order nonlinearity of silica compared to $As_2S_3$ and $As_2Se_3$.[13]

For both the chalcogenide glasses, we observe that the temporal shape of the THz-induced Kerr signal closely follows the intensity profile of the THz pulse (dashed, red curves). This is indicative of a very fast nonlinear response for the two glasses, and is typical for nonresonant excitation. In contrast to some liquid samples, such as $CH_2I_2$,[10] where the relaxation time can be rather long, there are no rotational dynamics of molecules in solid glasses. In the case of $As_2S_3$,

the THz-induced signal instantly responds to the changes in the intensity profile of the THz pulse, as there is good phase matching between the THz wave and probe beam in the glass. There is a slight indication of a delayed response from $As_2Se_3$. However, this might be due to the large velocity mismatch between the THz field and the optical probe, as will be discussed further below.

The analysis of the peak values of the THz-induced signal in glasses reveals a standard third-order nonlinear behavior, shown in Fig. 3. For the small values of the phase retardation observed here, the recorded values are accurately fitted by a quadratic fit $\Delta V/V_0 \approx \Delta\phi = k \times E^2$, where $k$ is a constant and $E$ is the electrical field strength. This demonstrates that the observed THz-induced signals in the chalcogenide samples are due to the Kerr effect ($\Delta n = \lambda K E^2$), where $\Delta n$ is the change in the refractive index, $\lambda$ is the wavelength, and $K$ is the Kerr constant. The nonlinear refractive index can be written as $n_2 = \Delta n/I$ where $I$ is the intensity of the THz pulse averaged over either the propagation length in the glass or the physical length of the sample, whichever is shorter.
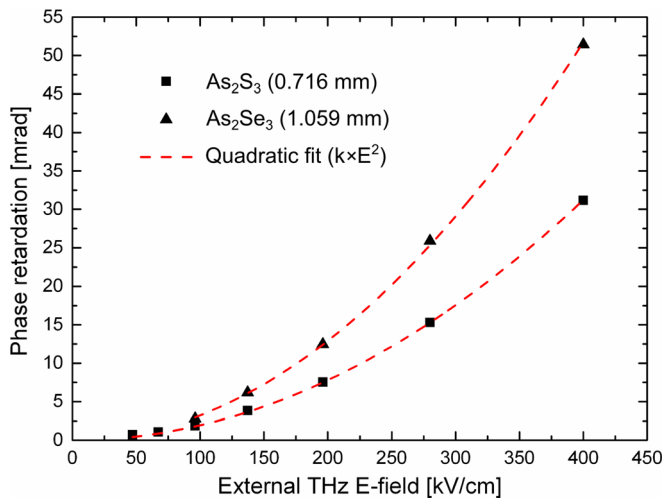
FIG. 3. The peak values of the THz-induced Kerr signals for $As_2S_3$ (squares) and $As_2Se_3$ (triangles). The red, dashed curves are quadratic fits to the measured data points.



FIG. 5. The refractive index (solid curves) and absorption coefficient (dashed curves) for $As_2S_3$ (red) and $As_2Se_3$ (black) samples as measured by THz-TDS.

As we have previously reported, chalcogenide glass has the universal characteristics of an amorphous system at lower terahertz frequencies with a monotonous increase of the absorption coefficient.[23] However, crystalline phases may exist within the amorphous matrix. To verify that our samples are truly amorphous, we performed the Kerr measurements with the full electrical THz field strength at different orientation angles of the $As_2S_3$ sample (Fig. 4). No significant change in the Kerr signal is observed when the sample was rotated from 0° to 90°.

To determine the magnitude of the Kerr effect, we measured both the refractive index and absorption coefficient of the two chalcogenide glasses in the terahertz range with a Picometrix T-Ray 4000 THz-TDS system, as shown in Fig. 5. The refractive indices for both glasses in the frequency range 0.2–1.0 THz are nearly constant (2.80 for $As_2S_3$ and 2.86 for $As_2Se_3$). The slightly higher $As_2Se_3$ refractive index can be explained by the higher density of $As_2Se_3$ (4.75 g/cm$^3$) compared to $As_2S_3$ (3.42 g/cm$^3$). The group indices for the 800-nm optical probe beam are 2.76[24] and

3.65[25] for $As_2S_3$ and $As_2Se_3$, respectively. The resulting velocity mismatch between the optical probe beam and the THz pulse may result in smearing of the recorded Kerr signals, and consequently a slight underestimation of the extracted nonlinear coefficient. This effect will be most profound for $As_2Se_3$. The absorption coefficient monotonously increases from nearly zero to approximately 20–22 cm$^{-1}$ for both samples between 0.2 THz and 1.0 THz. This behavior is universal for a wide range of glasses, and confirms the amorphous nature of chalcogenide glasses at low THz frequencies.[23,26] For further analysis, we calculated the weighted average of the absorption coefficient over the pulse spectrum in the range 0.2–1.0 THz. This range contains 84% of the total intensity of the THz pulse (see Fig. 1(b)). Averaged absorption coefficients $\alpha = 6.2$ cm$^{-1}$ and 10.8 cm$^{-1}$ are found for $As_2S_3$ and $As_2Se_3$ with a characteristic penetration depth ($L_{abs} = 1/\alpha$) of 1.61 mm and 0.93 mm, respectively. We use these values to calculate the local THz field inside the bulk sample taking absorption and Fresnel transmission coefficients into account.

We determined the THz-induced nonlinear refractive indices $n_2 = 1.746 \times 10^{-14}$ cm$^2$/W and $n_2 = 3.440 \times 10^{-14}$ cm$^2$/W at 800 nm for $As_2S_3$ and $As_2Se_3$, respectively, in Table I. The larger THz Kerr effect for $As_2Se_3$ is consistent with the significantly larger third-order nonlinear optical coefficient in $As_2Se_3$ as compared to $As_2S_3$.[5] The measured
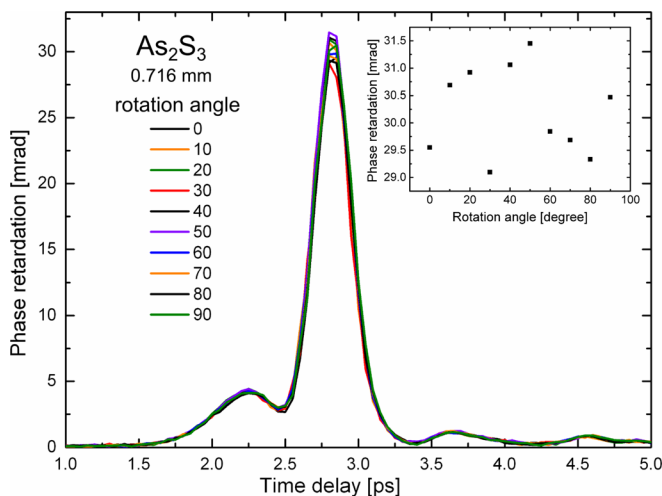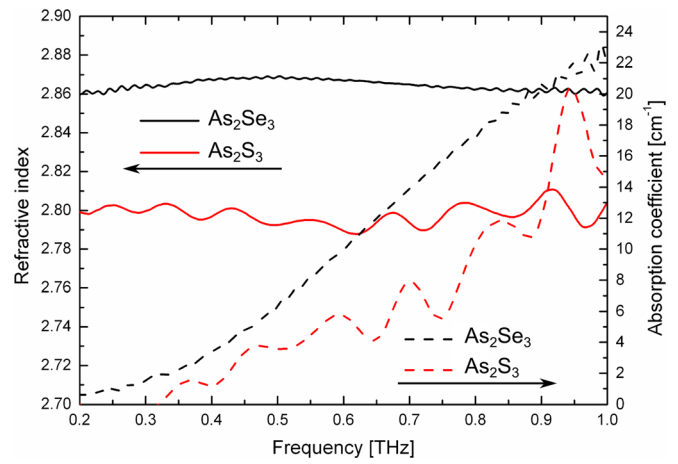


FIG. 4. The THz-induced Kerr signal as a function of $As_2S_3$ rotation angle at a THz electric field strength of 400 kV/cm. The rotation spans from 0° to 90° in steps of 10°.

TABLE I. THz-induced optical parameters of $As_2S_3$ and $As_2Se_3$ glasses.

|  | $As_2S_3$ | $As_2Se_3$ |
|---|---|---|
| $\Delta n^a$ [$10^{-6}$] | 5.34 | 6.30 |
| $n_2^b$ [$10^{-14}$ cm$^2$/W] | 1.75±0.09 | 3.44±0.17 |
| $n_{2,nir}^c$ [$10^{-14}$ cm$^2$/W] | 2.5 | 11.4 |
| $\chi^{(3)d}$ [$10^{-20}$ m$^2$/V$^2$] | 4.84±0.24 | 9.96±0.50 |
| $I_{peak}^e$ [$10^8$ W/cm$^2$] | 3.06±0.15 | 1.83±0.09 |

$^a\Delta n$ is the modulation of the refractive index.
$^b n_2$ is the nonlinear refractive index.
$^c n_{2,nir}$ is the nonlinear refractive index measured at near infrared.[12,14]
$^d\chi^{(3)}$ is the nonlinear susceptibility ($\chi^{(3)} = \frac{4}{3} \times \varepsilon_0 c \times n_0^2 n_2$, where $n_0$ is linear refractive index).
$^e I_{peak}$ is the peak intensity averaged through samples.

nonlinear refractive index for $As_2S_3$ is comparable with the values that were reported for the near infrared, $n_{2,nir} = 2.5 \times 10^{-14} \, cm^2/W$,[12] while that of $As_2Se_3$ is approximately 3 times lower, $n_{2,nir} = 11.4 \times 10^{-14} \, cm^2/W$.[14]

In summary, we have reported the observation of the THz-induced optical Kerr effect in solid materials, using intense THz pulses of up to $400 \, kV/cm$. Both chalcogenide samples, $As_2S_3$ and $As_2Se_3$, reveal large nonlinear refractive indices. Furthermore, due to the nonresonant nature of the third-order nonlinearity in the amorphous glasses, a near-instantaneous (faster than the time resolution of the experiment) response of the Kerr signal was observed.

[1] P. H. Siegel, IEEE Trans. Microwave Theory Tech. **52**, 2438 (2004).
[2] P. U. Jepsen, D. G. Cooke, and M. Koch, Laser Photonics Rev. **5**, 124 (2011).
[3] M. Tonouchi, Nat. Photonics **1**, 97 (2007).
[4] R. Frerichs, J. Opt. Soc. Am. **43**, 1153 (1953).
[5] A. Zakery, J. Non-Cryst. Solids **330**, 1 (2003).
[6] B. J. Eggleton, B. Luther-Davies, and K. Richardson, Nat. Photonics **5**, 141 (2011).
[7] J. Hebling, G. Almasi, I. Kozma, and J. Kuhl, Opt. Express **10**, 1161 (2002).
[8] H. Hirori, A. Doi, F. Blanchard, and K. Tanaka, Appl. Phys. Lett. **98**, 091106 (2011).
[9] S.-W. Huang, E. Granados, W. R. Huang, K.-H. Hong, L. E. Zapata, and F. X. Kärtner, Opt. Lett. **38**, 796 (2013).
[10] M. C. Hoffmann, N. C. Brandt, H. Y. Hwang, K.-L. Yeh, and K. A. Nelson, Appl. Phys. Lett. **95**, 231105 (2009).
[11] H. Y. Hwang, M. C. Hoffmann, N. C. Brandt, and K. A. Nelson, International Conference on Ultrafast Phenomena (2010).
[12] F. Smektala, C. Quemard, L. Leneindre, J. Lucas, A. Barthélémy, and C. De Angelis, J. Non-Cryst. Solids **239**, 139 (1998).
[13] J. M. Harbold, F. O. Ilday, F. W. Wise, J. S. Sanghera, V. Q. Nguyen, L. B. Shaw, and I. D. Aggarwal, Opt. Lett. **27**, 119 (2002).
[14] K. Ogusu, J. Yamasaki, S. Maeda, M. Kitao, and M. Minakata, Opt. Lett. **29**, 265 (2004).
[15] H. Kobayashi, H. Kanbara, M. Koga, and K. Kubodera, J. Appl. Phys. **74**, 3683 (1993).
[16] S. Madden, D.-Y. Choi, D. A. Bulla, A. V. Rode, B. Luther-Davies, V. G. Ta'eed, M. D. Pelusi, and B. J. Eggleton, Opt. Express **15**, 14414 (2007).
[17] S. Wong, M. Deubel, F. Pérez-Willard, S. John, G. A. Ozin, M. Wegener, and G. von Freymann, Adv. Mater. **18**, 265 (2006).
[18] T. Han, S. Madden, D. Bulla, and B. Luther-davies, Opt. Express **18**, 19286 (2010).
[19] Q. Wu and X.-C. Zhang, Appl. Phys. Lett. **67**, 3523 (1995).
[20] A. Nahata, D. H. Auston, T. F. Heinz, and C. Wu, Appl. Phys. Lett. **68**, 150 (1996).
[21] P. Jepsen, C. Winnewisser, M. Schall, V. Schyja, S. Keiding, and H. Helm, Phys. Rev. E **53**, R3052 (1996).
[22] Y.-S. Lee, *Principles of Terahertz Science and Technology* (Springer, Boston, MA, 2009).
[23] M. Zalkovskij, C. Zoffmann Bisgaard, A. Novitsky, R. Malureanu, D. Savastru, A. Popescu, P. Uhd Jepsen, and A. V. Lavrinenko, Appl. Phys. Lett. **100**, 031901 (2012).
[24] W. S. Rodney, I. H. Malitson, and T. A. King, J. Opt. Soc. Am. **48**, 633 (1958).
[25] C. Corrales, J. B. Ramírez-Malo, J. Fernández-Peña, P. Villares, R. Swanepoel, and E. Márquez, Appl. Opt. **34**, 7907 (1995).
[26] S. Taraskin, S. Simdyankin, S. Elliott, J. Neilson, and T. Lo, Phys. Rev. Lett. **97**, 055504 (2006).